JOURNAL OF GUIDANCE, CONTROL, AND DYNAMICS
Vol. 27, No. 4, July–August 2004

Formation Control of Satellites Subject to Drag Variations and J_2 Perturbations

David Mishne*
Technion—Israel Institute of Technology, 32000 Haifa, Israel

The issue of controlling the relative position of satellites in formation has acquired increasing attention in recent years. Special challenge is the control of a low-Earth-orbit formation, where differences in Earth oblateness effects and different atmospheric drag cause a drift of the relative position. A method is developed to compensate for the secular combined effects of first-order gravitational perturbations (J_2) and atmospheric drag perturbations. The compensation is performed by impulsive velocity corrections. The velocity correction vector and the timing of the correction are determined such that the secular drifts of the relative nodal rate and of the relative mean latitude rate are set to values that cancel out future drifts due to drag for the next time interval. In addition, an optimality condition is developed such that this correction velocity is minimized. After the correction, the orbital element deviations are not set to zero, but rather to small acceptable values for which the in-plane and the out-of-plane relative drifts are small and bounded. The algorithms for the determination of the velocity correction are developed, and a numerical example is presented. The effects of measurement noise and drag uncertainty are discussed as well.

Introduction

SEVERAL new space applications are based on operating a cluster of satellites in a close formation.[1] One of the key technologies involved in formation flying is the issue of the relative position control of the formation. In many cases, the objective is to keep the satellites in a desired relative formation, in the presence of natural perturbations. For low-Earth-orbit (LEO) satellites, the main perturbations are due to Earth oblateness, atmospheric drag, and solar radiation pressure. Usually, below 600-km altitude, the atmospheric drag is higher than the solar radiation pressure. These perturbations cause changes of the orbital elements of each satellite. In general, the effects of perturbations on each satellite are not the same; hence, a relative drift between the satellites is generated. Because of the Earth oblateness effect, small initial differences of the semimajor axis, eccentricity, and inclination between the satellites lead to different secular changes of both the nodal rate $\dot{\Omega}$ and the mean latitude rate $\dot{M} + \dot{\Omega}$. These differences lead to a buildup of the angular separation between the orbital planes of the satellites and of the in-plane angular separation. In addition, drag differences between the satellites cause different secular changes of the semimajor axis and the eccentricity, which in turn lead to different secular changes of the nodal rate and the mean latitude rate, due to Earth oblateness. The long-term combined effects of the perturbations result in relative drifts between the satellites, and corrections are needed to keep the desired pattern of the formation.

The issues of controlling the formation in the presence of Earth perturbations were discussed in previous research. Several researchers used the mean orbital elements for expressing and controlling the relative motion. Schaub and Alfriend[2] and Schaub et al.[3] defined J_2 invariant orbits by developing special relationships between the deviations of the mean orbital elements and developed nonlinear control laws to establish these orbits. Schaub and Alfriend[4] developed an impulsive control law by feeding back the relative differences in the mean orbital elements. Vadali et al.[5] developed control logic for a formation subject to Earth oblateness perturbations, using small periodic variations of the orbital elements. The solution method was based on periodic solution of Hill–Clohessy–Wiltshire equations. Folta and Quinn[6] developed a closed-loop control algorithm, based on online solution of the Lambert boundary value problem, to obtain the impulsive velocity corrections.

The effect of the drag force alone on the relative motion was investigated recently by several researchers. Mishne[7] modeled the drag force as quadratic in velocity and exponential with the altitude and used first-order expansion of this model in the Clohessy–Wiltshire equations. Carter and Humi[8] developed modified Clohessy–Wiltshire equations that included a quadratic drag force and obtained closed-form solution assuming that the density is inversely proportional to the altitude. In both cases, the model is restricted to small eccentricities.

The purpose of this paper is to develop a method for controlling the satellites by impulsive velocity corrections, such that the combined effect of the Earth oblateness and drag perturbations is compensated for while minimizing the fuel expenditure. The analysis will be based on the equations of the variations of the mean orbital elements; thus, it will not be restricted to small eccentricities. A method similar to Ref. 2 is adopted here, with two major additions: 1) inclusion of the relative drag and 2) addition of a new optimality condition to determine the velocity correction.

The basic requirement from the control logic is to cancel out the relative deviations of the mean drift of the nodal rate $\dot{\Omega}$ and the mean latitude rate $\dot{M} + \dot{\omega}$. Then all of the satellites in the formation will have equal drift of the mean values of these orbital elements. The correction is performed by a small impulsive velocity change. The velocity correction causes a step change in the instantaneous (osculating) orbital elements. In the paper, the conditions for the determination of the velocity corrections are derived. Two conditions are derived from the preceding requirements (similar to Ref. 2, but with the addition of drag), and a new third condition assures that the correction magnitude is minimal.

Analysis of the Relative Motion

A cluster of satellites is placed in a LEO. The formation of the cluster is designed such that the disturbance-free relative motion of the satellites is either fixed or periodic, without relative drift. Examples for such formations are the in-plane formation, the in-track formation, and the circular formation.[9] The perturbation-free

Presented as Paper 2002-4430 at the AIAA/AAS Astrodynamics Specialist Conference, Monterey, CA, 5–8 August 2002; received 28 October 2002; revision received 9 April 2003; accepted for publication 20 October 2003.

*Visiting Scientist, Asher Space Research Institute; on sabbatical from RAFAEL Armament Development Authority, Ltd.; davidm@tx.technion.ac.il. Associate Fellow AIAA.

position of an individual satellite is defined by a nominal set of orbital elements

$$\boldsymbol{\xi} = (a \quad e \quad i \quad \Omega \quad \omega \quad M)^T$$

where a is the semimajor axis, e the eccentricity, i the inclination, Ω the right ascension of ascending node, ω the argument of perigee, and M the mean anomaly.

In the presence of natural perturbations, the resulting orbit is represented by time-dependent elements of an osculating orbit. As discussed in the Introduction, the effects of the perturbations on each satellite are usually different, due to different $\boldsymbol{\xi}$ and different drag. Hence, the deviation of the element vector of each satellite from the nominal will lead to a relative perturbed orbit, which will eventually lead to a relative drift.

For LEO applications, the main natural perturbation sources are Earth oblateness, atmospheric drag, and solar radiation pressure. Here we shall limit the analysis to orbits below 400 km. For these orbits, the drag effect is much higher then the solar radiation effect. (For a typical satellite with drag coefficient of 2.2, orbiting the Earth at an altitude of 400 km, the drag force per unit area is 2.4×10^{-4} N/m^2, whereas the solar pressure, for a perfect reflector, is[10] 9×10^{-6} N/m^2.) Hence, the solar radiation effect will not be considered here.

If the effects of the perturbations on each satellite were identical, then the relative drift of the orbital elements would be zero. In this case, the formation would maintain the designed relative pattern, although its center of mass would be shifted from the nominal. However, the effect of both natural perturbations on each satellite is not identical. Each satellite has different drift of its orbital elements from the nominal; hence, a relative drift is built up. Here we shall track the relative position of the satellites through the orbital elements. Deviation of the mean latitude rate $\dot{M} + \dot{\omega}$ from the nominal indicates the in-plane angular deviation of the satellite from its nominal position. Deviation of the nodal rate $\dot{\Omega}$ from the nominal indicates the separation of the orbital plane from the nominal one. Hence, by limiting or nullifying the deviations of the relative rates of the specified orbital elements, the deviation of the relative position is controlled. We assume that the mission does not require a given predetermined set of relative orbital elements, but rather requires that the relative drift of the orbital elements are minimum.

First we develop the dynamics of the deviation of the orbital elements from the nominal due to Earth oblateness perturbation and due to drag difference. The mean change of the orbital elements, in the presence of Earth perturbations and atmospheric drag, is given by

$$\dot{\boldsymbol{\xi}} = \boldsymbol{A}(\boldsymbol{\xi}) \tag{1}$$

$\boldsymbol{A}$ is the 6×1 vector[10]

$$A_1 = -2\rho_p a^2 n K_D \left[I_0 + 2eI_1 + (3e^2/4)(I_0 + I_2) \right] \exp(-\beta a e)$$

$$A_2 = -\rho_p K_D a n \left[2I_1 + e(I_0 + I_2) - (e^2/4)(5I_1 + I_3) \right] \exp(-\beta a e)$$

$$A_3 = 0, \qquad A_4 = -\tfrac{3}{2} J_2 n (R_e/p)^2 \cos i$$

$$A_5 = \tfrac{3}{4} J_2 n (R_e/p)^2 (5\cos^2 i - 1)$$

$$A_6 = n + \tfrac{3}{4} J_2 n (R_e/p)^2 \sqrt{1-e^2}\,(3\cos^2 i - 1)$$

where ρ_p is the atmospheric density at the perigee, β the inverse of the atmospheric scale height, p the parameter of the orbit, n the mean motion, R_e the equatorial radius, J_2 the Earth oblateness coefficient, $K_D = SC_D/2m$ the drag factor, C_D the drag coefficient, and S the reference area of the drag coefficient.

The relationships for the averaged rates of the semimajor axis and of the eccentricity were developed for small eccentricity, expanding up to second-order power of e (Appendix A), in a method similar to obtaining the mean orbital elements for J_2 perturbation. The coefficients I_n are modified Bessel functions of the first kind, of order n and argument $\beta a e$.

As demonstrated by Eq. (1), the mean rates of the semimajor axis and of the eccentricity are affected by the drag, whereas the mean rates of the right ascension, the argument of perigee, and the mean anomaly are affected by Earth oblateness. The mean inclination is unaffected by either J_2 or by the drag (assuming nonrotating atmosphere); hence, $A_3 = 0$.

Initially, the orbital elements of the satellites are not necessarily identical. The initial deviations in a, e, or i cause a change in the secular drifts of Ω, ω, and M due to Earth oblateness, whereas the mean value of the inclination remains unchanged. In addition, we should expect small variations of the drag factors of the satellites due to different shapes and masses and different attitude profiles. This causes different secular changes of the semimajor axis and of the eccentricity, which in turn lead to different secular changes of the nodal rate and of the mean latitude rate, due to Earth oblateness. Next we calculate the dynamics of the deviation of the mean orbital elements from their nominal values, for an individual satellite.

Suppose that the initial orbital elements of an individual satellite are deviated slightly from the nominal by $\boldsymbol{\Delta\xi}_0$ and that the drag constant is deviated from the nominal by ΔK_D. The resulting deviations of the mean rates of change of the orbital elements are obtained by taking the variation of Eq. (1):

$$\Delta\dot{\boldsymbol{\xi}} = \boldsymbol{S}\Delta\boldsymbol{\xi} + \boldsymbol{G}\Delta K_D \tag{2}$$

where $\boldsymbol{S}$ is a 6×6 matrix obtained by $\boldsymbol{S} = \partial\boldsymbol{A}/\partial\boldsymbol{\xi}$ and $\boldsymbol{G}$ is a 6×1 vector obtained by $\boldsymbol{G} = \partial\boldsymbol{A}/\partial K_D$. The elements of $\boldsymbol{S}$ and $\boldsymbol{G}$ are given in Appendix B. Equation (2) is a linear representation of the dynamics of the deviations of the mean orbital elements from the nominal. Given an initial state deviation $\Delta\boldsymbol{\xi}_0$. and drag difference ΔK_D, the deviation of the mean element vector from the nominal is propagated according to Eq. (2).

To control and limit the deviation, impulsive velocity corrections are applied periodically. An impulsive velocity change $\boldsymbol{\Delta V}$, which is performed at time t, causes an instantaneous change of the orbital elements toward some desired value (yet unknown) $\Delta\boldsymbol{\xi}_d$. The relationship between the velocity change and the element change is given by Gauss's variational equations (see Ref. 10)

$$\boldsymbol{\Delta\xi}_d = \boldsymbol{\Delta\xi}(\nu) + \boldsymbol{B}(\xi, \nu)\boldsymbol{\Delta V} \tag{3}$$

where $\boldsymbol{B}(\xi, \theta)$ is the 6×3 matrix,

$$B_{11} = \frac{2e\sin\nu}{n\sqrt{1-e^2}}, \qquad B_{12} = \frac{2p}{nr\sqrt{1-e^2}}$$

$$B_{21} = \frac{\sqrt{1-e^2}\sin\nu}{na}, \qquad B_{22} = \frac{\sqrt{1-e^2}}{na}\left(\cos\nu + \frac{e+\cos\nu}{1+e\cos\nu}\right)$$

$$B_{33} = \frac{r\cos\nu}{na^2\sqrt{1-e^2}}, \qquad B_{43} = \frac{r\sin\nu}{na^2\sqrt{1-e^2}\sin i}$$

$$B_{51} = -\frac{\sqrt{1-e^2}\cos\nu}{nae}, \qquad B_{52} = \frac{\sqrt{1-e^2}\sin\nu}{nae}\left(1 + \frac{r}{p}\right)$$

$$B_{53} = -\frac{r\cos i\sin\nu}{h\sin i}$$

$$B_{61} = \frac{p\cos\nu - 2er}{na^2 e}, \qquad B_{62} = -\frac{(p+r)\sin\nu}{na^2 e}$$

All of the other elements of $\boldsymbol{B}$ are zero. Here ν is the true anomaly at the instant of correction. The components of $\boldsymbol{\Delta V}$ are Δu along the direction of the radius, Δv perpendicular to the radius in the orbit plane and in the direction of the motion, and Δw normal to the orbit plane.

The orbital elements in Eq. (3) are the osculating elements. As discussed in previous research,[3,4] the changes in the osculating orbital elements are directly reflected in corresponding changes of the mean orbital elements. Hence, computing the $\boldsymbol{B}$ matrix using the mean orbital elements is consistent with the small perturbation concept. Note that several terms in the $\boldsymbol{B}$ matrix are singular for $e = 0$ or $i = 0$; therefore, this method is not valid for pure circular or pure equatorial orbits.

Determination of the Velocity Correction

To limit the drift of each satellite from the nominal, we require that the orbital elements immediately following the correction will have values such that the changes of $\dot{\Omega}$ and $\dot{\omega}+\dot{M}$ from the nominal are set to desired values. The velocity correction $\boldsymbol{\Delta V}$ is chosen then such that the two following conditions are met:

$$\Delta\dot{\Omega} = \Delta\dot{\Omega}_d, \qquad \Delta(\dot{M}+\dot{\omega}) = \Delta(\dot{M}+\dot{\omega})_d$$

where $\Delta\dot{\Omega}_d$ and $\Delta(\dot{M}+\dot{\omega})_d$ are the desired drifts of Ω and $(M+\omega)$, respectively. If there is no drag difference, the desired drift rates are set to zero (as discussed in Ref. 2). In this case, the corrected deviation of the orbital parameters (Δa_d, Δe_d and Δi_d), as calculated from Eq. (3), would remain theoretically unchanged, and no further correction is needed. However, when drag difference exists, the corrected element deviation $\Delta\boldsymbol{\xi}_d$ is an initial value and the deviation continues to change according to Eq. (2). The orbital elements deviate from the J_2 invariant values and drifts in Ω and $(M+\omega)$ are accumulated, and after some time, further velocity correction should be applied. The desired drift rates $\Delta\dot{\Omega}_d$ and $\Delta(\dot{M}+\dot{\omega})_d$ are, therefore, not set to zero, but rather are set to values that will compensate for the effect of the drag difference, in a manner explained in the sequel.

By combining Eqs. (2) and (3), we get the following two conditions for the velocity correction:

$$\begin{aligned}\boldsymbol{L}_1(\boldsymbol{B}\Delta\boldsymbol{V}+\boldsymbol{\Delta\xi}) + G_4\Delta K_D &= \Delta\dot{\Omega}_d\\ \boldsymbol{L}_2(\boldsymbol{B}\Delta\boldsymbol{V}+\boldsymbol{\Delta\xi}) + (G_5+G_6)\Delta K_D &= \Delta(\dot{M}+\dot{\omega})_d\end{aligned} \tag{4}$$

where the vector $\boldsymbol{L}_1$ is the fourth row of the $\boldsymbol{S}$ matrix, $\boldsymbol{L}_2$ is the sum of the fifth and sixth rows of the $\boldsymbol{S}$ matrix, and G_i are elements of the $\boldsymbol{G}$ vector (Appendix B).

Rewriting Eqs. (4) as two planes in the velocity correction space (Δu, Δv, and Δw), we obtain

$$\begin{aligned}g_1(\Delta u, \Delta v, \Delta w, \nu) &= N_{11}\Delta u + N_{12}\Delta v + N_{13}\Delta w + N_{14} = 0\\ g_2(\Delta u, \Delta v, \Delta w, \nu) &= N_{21}\Delta u + N_{22}\Delta v + N_{23}\Delta w + N_{24} = 0\end{aligned} \tag{5}$$

where the elements of the $\boldsymbol{N}$ matrix are easily determined by expanding Eqs. (4). Performing the expansion, and keeping only the nonzero elements of $\boldsymbol{S}$, $\boldsymbol{B}$, and $\boldsymbol{G}$, we obtain

$$N_{11} = S_{41}B_{11} + S_{42}B_{21}, \qquad N_{12} = S_{41}B_{12} + S_{42}B_{22}$$

$$N_{13} = S_{43}B_{33}, \qquad N_{14} = S_{41}\Delta a + S_{42}\Delta e + S_{43}\Delta i - \Delta\dot{\Omega}_d$$

$$N_{21} = (S_{51}+S_{61})B_{11} + (S_{52}+S_{62})B_{21}$$

$$N_{22} = (S_{51}+S_{61})B_{12} + (S_{52}+S_{62})B_{22}$$

$$N_{23} = (S_{53}+S_{63})B_{33}$$

$$N_{24} = (S_{51}+S_{61})\Delta a + (S_{52}+S_{62})\Delta e + (S_{53}+S_{63})\Delta i - \Delta(\dot{M}+\dot{\omega})_d$$

The drag factor deviation ΔK_D does not appear explicitly in the preceding equations (because G_4, G_5, and G_6 are zero). However, it appears implicitly because the deviations Δa and Δe depend on ΔK_D according to Eq. (2). In addition, the choice of the desired drifts is based on ΔK_D, as explained later.

Equations (5) form two linear equations for the three components of the desired velocity correction $\boldsymbol{\Delta V}$. A third equation is obtained by requiring that the velocity correction be minimal. The geometrical interpretation of condition (5) is that the velocity correction vector should touch the intersection line of the two planes $g_1(\Delta u, \Delta v, \Delta w) = 0$ and $g_2(\Delta u, \Delta v, \Delta w) = 0$. From all possible solutions, the minimum correction is the vector $(\Delta u, \Delta v, \Delta w)$ that is perpendicular to the intersection line. The mathematical condition is then

$$(\Delta g_1 \times \Delta g_2)\cdot\Delta\boldsymbol{V} = 0$$

where Δg_i is the gradient of each equation in Eqs. (5). Expanding this equation yields

$$N_{31}\Delta u + N_{32}\Delta v + N_{33}\Delta w = 0 \tag{6}$$

where the elements N_{3j} are easily computed from the N_{ij} elements in Eqs. (5):

$$N_{31} = N_{12}N_{23} - N_{22}N_{13}, \qquad N_{32} = N_{13}N_{21} - N_{11}N_{23}$$

$$N_{33} = N_{11}N_{22} - N_{12}N_{21}$$

Equations (5) and (6) form three linear equations for the components of the velocity correction vector. The solution is

$$\Delta\boldsymbol{V}(\nu) = \boldsymbol{N}_A^{-1}\boldsymbol{N}_B \tag{7}$$

The 3×3 matrix $\boldsymbol{N}_A$ is composed of the first three columns of $\boldsymbol{N}$, and the vector $\boldsymbol{N}_B$ is the negative of the last column of $\boldsymbol{N}$, with $\boldsymbol{N}_{34} = 0$. Equation (7) is equivalent to the minimum-norm solution of Eq. (5).

The velocity correction obtained by Eq. (7) is a function of the true anomaly ν. For arbitrary initial state deviation $\Delta\boldsymbol{\xi}_0$, the best point where the correction should be applied (the minimum velocity correction) is located at some point on the trajectory. To find this best point, we find numerically the minimum value of the correction magnitude in the time period specified by $\nu_0 < \nu < \nu_{\max}$:

$$\Delta\boldsymbol{V}_{\min} = \min_{\nu}|\Delta\boldsymbol{V}(\nu)| \tag{8}$$

The value of $\nu_{\max}$ is consistent with the maximum allowed deviation of the orbital parameters, bounded by the value $\nu_0 + 2\pi$. The resulting orbital element deviations immediately following the correction, $\Delta\boldsymbol{\xi}_d$, are determined from Eq. (3), using the correction vector $\Delta\boldsymbol{V}_{\min}$.

As discussed before, if there were no drag difference, the corrected element deviations Δa_d, Δe_d, and Δi_d, would theoretically remain unchanged, and no further correction is needed. However, when drag difference exists, the elements Δa and Δe slowly deviate from the J_2 invariant values, and after some time, further velocity correction should be applied. The time interval between subsequent corrections is chosen according to the allowed deviation. Define this time interval as T, the values of the orbital elements deviations at this time, just before the velocity correction, are obtained by solving the linear dynamics [Eq. (2)]. The deviation due to drag difference only is given by[11]

$$\Delta\boldsymbol{\xi}_{\text{drag}}(T) = \int_0^T \exp[\boldsymbol{S}(t-\tau)]\boldsymbol{G}\Delta K_d\,\mathrm{d}\tau \tag{9}$$

The fourth element of $\Delta\boldsymbol{\xi}_{\text{drag}}(T)$ is the drift of Ω due to drag, $\Delta\Omega_{\text{drag}}(T)$, and the sum of the fifth and sixth elements is the drift of $M+\omega$ due to drag, $\Delta[M(T)+\omega(T)]_{\text{drag}}$. The desired drifts immediately following the velocity correction, $\Delta\dot{\Omega}_d$ and $\Delta(\dot{M}+\dot{\omega})_d$, will be chosen to be in the opposite direction of the expected drift due to drag that will be accumulated till the next correction:

$$\begin{aligned}\Delta\dot{\Omega}_d &= -\Delta\Omega_{\text{drag}}(T)/T\\ \Delta(\dot{M}+\dot{\omega})_d &= -\Delta[M(T)+\omega(T)]_{\text{drag}}/T\end{aligned} \tag{10}$$

These values will be used in Eq. (4). The velocity correction will result then in an initial drift rate, which is opposite to the drift due to drag, resulting in a net zero drift at the end of the time interval T.

The desired drift rates $\Delta\dot{\Omega}_d$ and $\Delta(\dot{M}+\dot{\omega})_d$. are obtained using Eq. (9), or, alternatively, using the following linear approximation, valid for short time interval T between corrections:

$$\Delta\dot{\Omega} = S_{41}\Delta a + S_{42}\Delta e = \left(S_{41}\frac{\partial a}{\partial K_d} + S_{42}\frac{\partial e}{\partial K_d}\right)\Delta K_d$$

$$= \left(S_{41}\frac{\partial A_1}{\partial K_d} + S_{42}\frac{\partial A_2}{\partial K_d}\right)\Delta K_d t = (S_{41}A_1 + S_{42}A_2)\frac{\Delta K_d}{K_d}t$$

At time T,

$$\Delta\Omega(T) = \tfrac{1}{2}(S_{41}A_1 + S_{42}A_2)(\Delta K_d/K_d)T^2$$

and similarly,

$$\Delta M(T)+\Delta\omega(T) = \tfrac{1}{2}[(S_{51}+S_{61})A_1+(S_{51}+S_{61})A_2](\Delta K_d/K_d)T^2$$

Summary of the Control Procedure

At time t_0 we have an initial value of the state deviation from the nominal $\Delta\boldsymbol{\xi}_0$. and an estimate of the drag deviation ΔK_D. The state deviation $\Delta\boldsymbol{\xi}_0$. can be estimated from measurements of relative position and velocity. The drag deviation can be estimated from past measurements of the position using the method explained and demonstrated in Ref. 7. Equation (2) is then propagated to yield the predicted deviation of the orbital elements for a given time interval. This time interval should be consistent with the maximum allowed deviation of the satellite from the nominal. The desired drift rates are determined according to Eqs. (9) and (10). The velocity correction and the timing of the correction are determined from Eqs. (7) and (8). The relationship between the time variable and the true anomaly is determined from the time equation (Kepler equation). Then at time t_0, we have a predetermined value of the velocity correction and the timing of the correction. When the predetermined correction time is reached, the velocity correction is recalculated from Eq. (7) using the actual values of Δa, Δe, and Δi as obtained from measurements. From this point on, the deviations of the orbital parameters from the nominal (which increase continuously due to the effect of the drag deviation) are monitored. When the deviation exceeds the maximum allowed, a new velocity correction [obtained by Eq. (7)] is performed. Each velocity correction sets the drift rate to a value that cancels out future drifts due to drag for the next time interval. The resulting accumulating deviations of $\Delta\Omega$ and $\Delta(\omega + M)$ will be close to zero, with the addition of errors due to noisy measurements and drag uncertainty.

Effect of Measurement Errors

As already discussed, the evaluation of the velocity correction impulses is performed using estimates of the relative deviations of the orbital elements Δa, Δe, and Δi. This estimation is usually based on noisy measurements of relative position and velocity; hence, the estimated orbital elements contain errors. How and Tillerson[12] investigated the effect of measurement errors of relative position and velocity on the performance of a formation that follows a planned trajectory, starting from nominal initial conditions. Their results showed that measurement errors, and in particular the relative velocity error, may have a significant effect on the performance. In the present case, errors in the estimation of the relative orbital elements will result in a residual drift of $\Delta\Omega$ and $\Delta(\omega + M)$. Next we develop relations to estimate this residual drift.

Let us rewrite Eq. (7) to reflect the linear relationship between the correction velocity impulse to the deviation of the orbital element vector $\Delta\boldsymbol{\xi}$:

$$\Delta\boldsymbol{V}(\nu) = \boldsymbol{N}_A^{-1}\boldsymbol{N}_c\Delta\boldsymbol{\xi} + \boldsymbol{N}_A^{-1}\begin{bmatrix}\Delta\dot{\Omega}_d\\ \Delta(\dot{M}+\dot{\omega})_d\\ 0\end{bmatrix} \tag{11}$$

where $\boldsymbol{N}_c$ is a 3×6 matrix, with the first row equal to the negative $\boldsymbol{L}_1$ vector, the second row equal to the negative $\boldsymbol{L}_2$ vector, and the third row a zero vector.

Denoting the estimation error of the orbital elements vector as $\boldsymbol{\varepsilon}_\xi$, and the resulted residual drift of $\Delta\Omega$ and $\Delta(\omega + M)$ as $\varepsilon_{\dot{\Omega}}$ and $\varepsilon_{\dot{\omega}+\dot{M}}$, respectively, and using Eqs. (4) and (11), we obtain

$$\begin{aligned}\Delta\dot{\Omega} + \varepsilon_{\dot{\Omega}} &= \boldsymbol{L}_1\left[\boldsymbol{B}\boldsymbol{N}_A^{-1}\boldsymbol{N}_c(\boldsymbol{\Delta\xi}+\boldsymbol{\varepsilon}_\xi)+\boldsymbol{\Delta\xi}\right]\\ &\quad+\boldsymbol{L}_1\boldsymbol{B}\boldsymbol{N}_A^{-1}[\Delta\dot{\Omega}_d \quad \Delta(\dot{M}+\dot{\omega})_d \quad 0]^T\\ \Delta(\dot{\omega}+\dot{M}) + \varepsilon_{\dot{\omega}+\dot{M}} &= \boldsymbol{L}_2\left[\boldsymbol{B}\boldsymbol{N}_A^{-1}\boldsymbol{N}_c(\boldsymbol{\Delta\xi}+\boldsymbol{\varepsilon}_\xi)+\boldsymbol{\Delta\xi}\right]\\ &\quad+\boldsymbol{L}_2\boldsymbol{B}\boldsymbol{N}_A^{-1}[\Delta\dot{\Omega}_d \quad \Delta(\dot{M}+\dot{\omega})_d \quad 0]^T\end{aligned} \tag{12}$$

Remembering that the correction is such that $\Delta\dot{\Omega} = \Delta\dot{\Omega}_d$ and $\Delta(\dot{\omega}+\dot{M}) = \Delta(\dot{\omega}+\dot{M})_d$, we obtain the relationships between the residual drifts to the estimation errors of the orbital elements:

$$\begin{aligned}\varepsilon_{\dot{\Omega}} &= \boldsymbol{L}_1\boldsymbol{B}\boldsymbol{N}_A^{-1}\boldsymbol{N}_c\boldsymbol{\varepsilon}_\xi = -\boldsymbol{L}_1\boldsymbol{\varepsilon}_\xi\\ \varepsilon_{\dot{\omega}+\dot{M}} &= \boldsymbol{L}_2\boldsymbol{B}\boldsymbol{N}_A^{-1}\boldsymbol{N}_c\boldsymbol{\varepsilon}_\xi = -\boldsymbol{L}_2\boldsymbol{\varepsilon}_\xi\end{aligned} \tag{13}$$

The error of the estimation of the orbital elements, $\boldsymbol{\varepsilon}_\xi$, is obtained from the errors of the actual measurements. When carrier-phase differential global positioning system (GPS) is used, it is possible to obtain precise relative measurements of relative position and velocity.[13,14] From these measurements, the orbital elements can be estimated in various methods.[15] The transformation from the measurement errors of position and velocity to the estimated errors of the orbital elements is given in Appendix C. Using this transformation, and using Eq. (13), we obtain the residual drift of Ω due to the measurement noise,

$$\begin{aligned}\varepsilon_{\Delta\dot{\Omega}\_r} &= -\left(S_{41}\frac{\partial a}{\partial r} + S_{42}\frac{\partial e}{\partial r} + S_{43}\frac{\partial i}{\partial r}\right)\varepsilon_r\\ \varepsilon_{\Delta\dot{\Omega}\_V} &= -\left(S_{41}\frac{\partial a}{\partial V} + S_{42}\frac{\partial e}{\partial V} + S_{43}\frac{\partial i}{\partial V}\right)\varepsilon_{Vr}\end{aligned} \tag{14}$$

where ε_r and ε_V, are the measurement errors of relative position and relative velocity, respectively, and $\varepsilon_{\Delta\dot{\Omega}\_r}$ and $\varepsilon_{\Delta\dot{\Omega}\_V}$ are the residual drift of $\Delta\Omega$ due to measurement errors in r and V, respectively. The partials $\partial a/\partial r$, etc., in Eq. (14) are defined in Appendix C.

Because the measurement errors ε_r and ε_V are independent, we calculate the combined residual drift using root-sum-square summation:

$$\varepsilon_{\Delta\dot{\Omega}} = \sqrt{\varepsilon^2_{\Delta\dot{\Omega}\_r} + \varepsilon^2_{\Delta\dot{\Omega}\_V}} \tag{15}$$

Similar expression can be written for the residual drift $\varepsilon_{\Delta(\dot{\omega}+\dot{M})}$. Numerical results are given in the next section.

Results

The method is demonstrated for a formation of small satellites. Each satellite has nominal mass of 100 kg, effective cross section area of 1 m^2, and nominal drag coefficient $C_D = 2.2$. The nominal orbital elements are $a = 6700$ km, $e = 0.004$, $i = 48$ deg, $\omega = 10$ deg, $\Omega = 0$, $M = 120$ deg.

First we calculate the angular uncorrected deviation of the orbital plane from the nominal one, due to estimated drag deviation of 10% from the nominal, combined with J_2 perturbation.

If the initial orbital elements are nominal, the orbit conserves the nominal inclination angle. The deviation of the right ascension of ascending node from the nominal, $\Delta\Omega$, due to the drag deviation, is obtained by solving Eq. (2). The angular deviation of the orbital plane is calculated from the spherical relationship

$$\cos\Delta\alpha = \cos^2 i + \sin^2 i\cos\Delta\Omega$$

where $\Delta\alpha$ is the angular deviation of the orbital plane from the nominal.

This angular deviation as a function of the number of orbits is shown in Fig. 1. The angle accumulated after 100 orbits (about 6 days) is 0.0730 deg. For this angle, the maximum distance of the satellite from the nominal plane is 8.56 km.

The angular in-plane deviation from the nominal, calculated by $\Delta\psi = \Delta\Omega\cos i + \Delta(\omega + M)$, is in Fig. 2. The angular deviation after five orbits is about 0.1 deg, which is equivalent to a distance of about 11.5 km.

Next we demonstrate the implementation of the proposed correction method. We choose a correction interval of one orbit. For this time interval, we predict the expected drift due to the estimated drag deviation, which determines the desired values $\Delta\dot{\Omega}_d$ and $\Delta(\dot{M}+\dot{\omega})_d$. [Eqs. (9) and (10)]. The results for the velocity

Table 1 Velocity corrections required to cancel out the secular differential drift in $\dot{\Omega}$ and in $\dot{\omega}+\dot{M}$

Initial element deviations[a]	Drag deviation,[a] %	Optimal velocity correction,[b] m/s	Element deviations[c]
		Case 1	
$da_0=-0.1$ km	0	$\Delta u=-0.000036$	$\Delta a_d=-2.55\times10^{-5}$ km
$de_0=0.0001$		$\Delta v=0.058$	$\Delta e_d=8.5\times10^{-5}$
$di_0=0.005$ deg		$\Delta w=0.661$	$\Delta i_d=7.1\times10^{-5}$ deg
		$\Delta V_{\text{tot}}=0.663$	
		Case 2	
$da_0=-0.1$ km	10	$\Delta u=0.0000365$	$\Delta a_d=0.0483$ km
$de_0=0.0001$		$\Delta v=0.0850$	$\Delta e_d=1.22\times10^{-4}$
$di_0=0.005$ deg		$\Delta w=-0.662$	$\Delta i_d=1.0\times10^{-4}$ deg
		$\Delta V_{\text{tot}}=0.668$	
		Case 3[d]	
$da_0=-0.1$ km	10	$\Delta u=0.0000361$	$\Delta a_d=-3.46\times10^{-5}$ km
$de_0=0.0001$		$\Delta v=0.0573$	$\Delta e_d=1.15\times10^{-4}$
$di_0=0.005$ deg		$\Delta w=-0.663$	$\Delta i_d=0.96\times10^{-4}$ deg
		$\Delta V_{\text{tot}}=0.665$	

[a]From the nominal.
[b]Required to cancel out the secular drift in $\dot{\Omega}$ and in $\dot{\omega}+\dot{M}$.
[c]From the nominal immediately after the correction.
[d]Drag not accounted for.

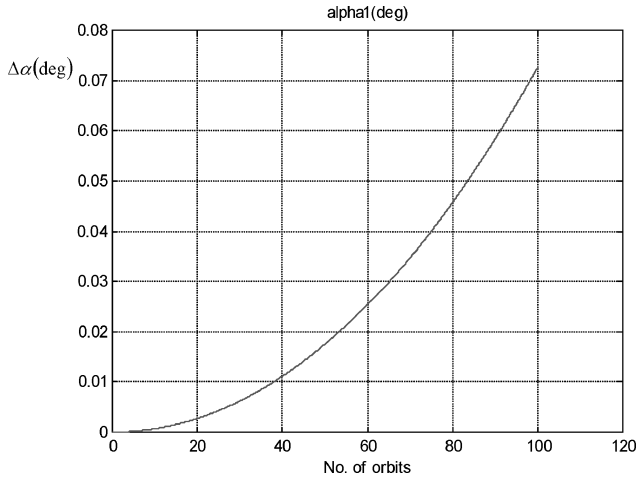

Fig. 1 Angular deviation of the orbital plane from the nominal, no correction.

correction for several combinations of initial element deviations and drag deviation are presented in Table 1.

The first case includes arbitrary initial element deviations, with no drag deviation. The second case includes both initial element deviations and drag deviations. The third case has same initial conditions and drag deviation as in case 2, but the correction does not account for the drag deviation, that is, $\Delta\dot{\Omega}_d$ and $\Delta(\dot{M}+\dot{\omega})_d$ are set to zero in the algorithm. The velocity correction that is necessary to obtain the desired drifts was calculated using the proposed method and is given in Table 1.

The element deviations from the nominal immediately following the correction are outlined in Table 1. For case 1 (no drag deviation), the resulted value of Δa_d is extremely small, essentially zero. This is expected, because to keep the in-plane drift minimal, the period must be close to the nominal. The values of Δe_d and Δi_d are also small, but the transformation of those element deviations to distance deviations is on the order of tens to hundreds of meters.

For case 2, the resulted value of Δa_d. is about 38 m. This causes an initial drift rate that compensates for the predicted drift due to drag deviation, such that at the end of the time interval the net drift is zero. Because drag deviation still exists, the drift continues to accumulate, and further periodic corrections are necessary at the following time intervals.

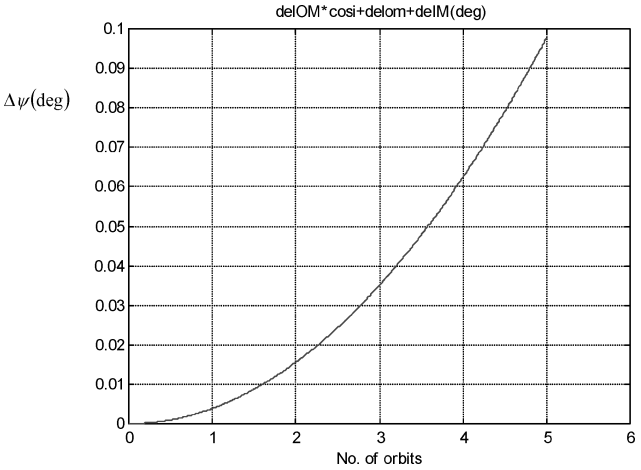

Fig. 2 In-plane angular deviation from the nominal, no correction.

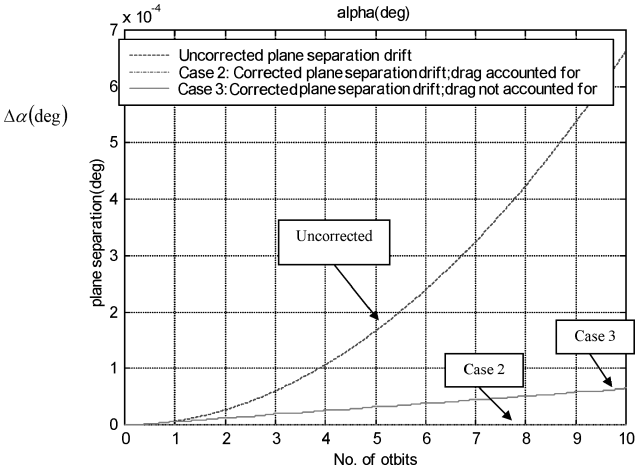

Fig. 3 Angular deviation of the orbital plane from the nominal with corrections.

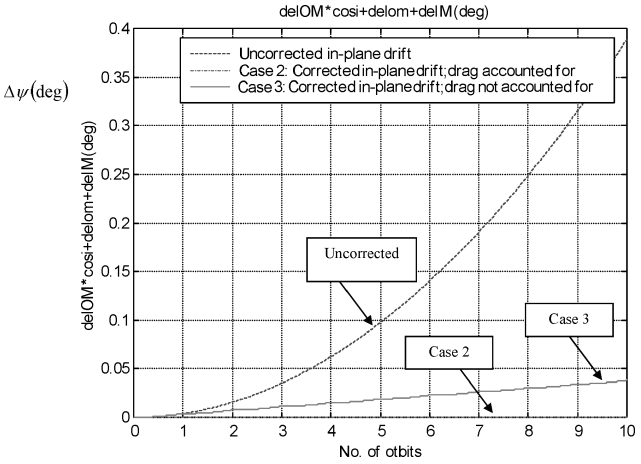

Fig. 4 In-plane angular deviation from the nominal with corrections.

The in-plane drift $\Delta\psi$ and the out-of-plane drift $\Delta\alpha$ for the various cases are in Figs. 3 and 4, together with the uncorrected drifts, for duration of 10 consecutive orbits, with velocity corrections applied after each orbit. Case 2 represents the complete correction: Each velocity correction sets the elements such that the initial drifts of Ω and $(M+\omega)$ compensate for the drift due to drag that would be accumulated during the following time interval, till the next correction. Case 3 represents partial correction: Each velocity correction sets the elements such that the initial drift of the preceding elements is zero. This case also demonstrates the effect of 100% uncertainty of the estimated drag deviation ΔK_D.

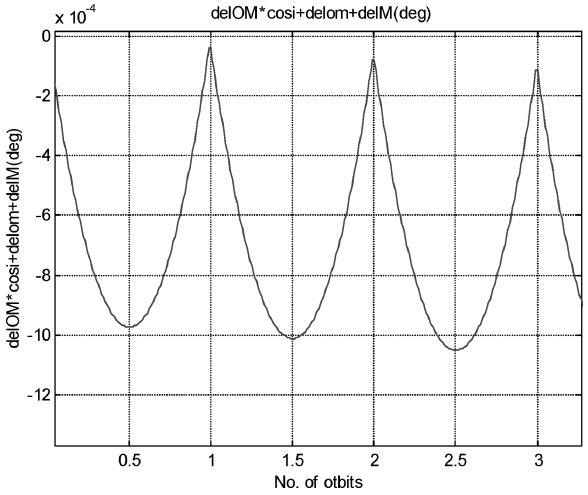

Fig. 5 In-plane angular deviation from the nominal with corrections, enlargement of case 2.

As demonstrated in Figs. 3 and 4, the complete correction (case 2) results in almost zero drift. In case 3 (100% drag estimation uncertainty), the drift is not zero, but is much smaller than the uncorrected case (about 1/10th of the uncorrected case). Figure 5 is an enlargement of case 2 shown in Fig. 4 and shows the near-zero behavior of the drift. The magnitude of the relative deviation in the in-plane angle $\Delta\psi$ is almost bounded by 10^{-3} deg, and the drift is stopped.

Residual Drift Due to Measurement Errors

The velocity correction impulse sets the nominal drift to the desired value. However, due to measurement errors, there is a residual drift, as discussed in earlier sections. Here we determine this residual drift for the preceding example, using realistic measurement errors of the relative position and relative velocity. According to results presented in Ref. 13, carrier-phase differential GPS measurement results in relative position error of about 10 mm in each axis and relative velocity error of about 2 mm/s in each axis. In Ref. 14, even better accuracy of the relative velocity is reported. For the present example, we use the conservative values: rss errors of 17 mm in the relative position and 3.4 mm/s for the relative velocity. Using these values in Eqs. (14) and (15), we obtain the residual drift after one orbit (radian per second):

$$\varepsilon_{\Delta\dot{\Omega}} = 4.07 \times 10^{-12}, \qquad \varepsilon_{\Delta(\dot{M}+\dot{\omega})} = 1.54 \times 10^{-9}$$

These residual drifts cause residual errors in the out-of-plane angular deviation $\Delta\alpha$ and the in-plane angular deviation $\Delta\psi$. The errors after one orbit are

$$\varepsilon_{\Delta a} = 1.65 \times 10^{-8} \text{ rad} = 9.46 \times 10^{-7} \text{ deg}$$

$$\varepsilon_{\Delta\psi} = 8.4 \times 10^{-6} \text{ rad} = 0.00048 \text{ deg}$$

Increasing the rate of corrections, that is, shorter time intervals between corrections, can reduce these errors.

Conclusions

A method for controlling the relative formation of LEO satellites, subject to Earth perturbations and having different drag effects, was developed. The control approach is based on periodical impulsive velocity corrections. Each velocity correction is determined such that the element deviations following the correction are set to small acceptable values for which the relative secular drift of nodal rate $\dot{\Omega}$ and the mean latitude rate $\dot{M}+\dot{\omega}$ are opposite to the expected drifts due to drag deviation that will be accumulated till the next correction. In addition to these two conditions, a condition for choosing the minimum velocity correction was developed; thus, a unique velocity correction vector is obtained.

The method was demonstrated for a LEO formation in almost circular orbit with average altitude of 322 km. The results showed that the in-plane drift and the out-of-plane drift, due to the combined effects of J_2 and drag difference, are set almost to zero. Measurements of the relative position and velocity, as well as estimation of the drag difference, are required to obtain the correction vector. Errors in those measurements cause residual errors in the drifts that can be estimated. To reduce these errors, the time interval between consecutive correction is reduced.

Appendix A: Mean Change of the Orbital Elements Due to Drag

Here we neglect the rotation of the atmosphere. Following this assumption, the inclination and the right ascension of ascending node are not affected by the drag. The instantaneous rates of change of the semimajor axis and the eccentricity and the argument of perigee due to atmospheric drag are obtained from Gauss's variation of parameters equations,[10] with the drag force, which acts along the negative tangent to the orbit, as the only perturbation:

$$\dot{a} = -(2a/r)(2a-r)\rho V K_d, \qquad \dot{e} = -2(\cos\nu + e)\rho V K_d$$

$$\dot{\omega} = -(2\sin\nu/e)\rho V K_d$$

To determine the mean value, we average $\mathrm{d}\xi/\mathrm{d}\theta$ over one orbit:

$$\left(\frac{\mathrm{d}\xi}{\mathrm{d}t}\right)_{\text{av}} = \frac{n}{2\pi}\int_0^{2\pi}\frac{\dot{\xi}}{\dot{\nu}}\,\mathrm{d}V$$

The atmospheric density is modeled as $\rho = \rho_p e^{-\beta(r-r_p)}$, where β is the inverse of the atmospheric scale height, which is assumed to be constant in the altitude range between perigee and apogee.

Because $(\dot{\omega}/\dot{\nu})$ is symmetric with respect to ν, the mean change of ω is zero. The mean rates of change of the semimajor axis and of the eccentricity have secular values, which are given by Vallado,[10]

$$\dot{a}_{\text{av}} = -2\rho_p a^2 n K_D\left\{I_0(\beta ae) + 2eI_1(\beta ae) + (3e^2/4)[I_0(\beta ae) + I_2(\beta ae)] + \mathcal{O}(e^3)\right\}\exp(-\beta ae)$$

$$\dot{e}_{\text{av}} = -\rho_p K_D a n\left\{2I_1(\beta ae) + e[I_0(\beta ae) + I_2(\beta ae)] - (e^2/4)[5I_1(\beta ae) + I_3(\beta ae)] + \mathcal{O}(e^3)\right\}\exp(-\beta ae)$$

where $I_n(\beta ae)$ are modified Bessel functions of the first kind, defined in integral form (see Ref. 16),

$$I_n(z) = \frac{1}{2\pi}\int_0^{2\pi} e^{z\cos\theta}\cos(n\theta)\,\mathrm{d}\theta$$

Appendix B: Elements of *S* and *G*

The elements of the ***S*** matrix are found by direct differentiation of the ***A*** vector with respect to each one of the state variables:

$$S_{11} = \frac{\partial A_1}{\partial a} = -\sqrt{\frac{\mu}{a}}K_d\rho_p\left(f_1 + 2a\frac{\partial f_1}{\partial a}\right)$$

$$S_{12} = \frac{\partial A_1}{\partial e} = -2\sqrt{\mu a}K_d\rho_p\frac{\partial f_1}{\partial e}$$

$$S_{21} = \frac{\partial A_2}{\partial a} = \frac{1}{2}\sqrt{\frac{\mu}{a^3}}K_d\rho_p\left(f_2 - 2a\frac{\partial f_2}{\partial a}\right)$$

$$S_{22} = \frac{\partial A_2}{\partial e} = -\sqrt{\frac{\mu}{a}}K_d\rho_p\frac{\partial f_2}{\partial e}$$

$$S_{41} = \frac{\partial A_4}{\partial a} = \frac{21}{4}J_2\left(\frac{R_e}{p}\right)^2\frac{n}{a}\cos i$$

$$S_{42} = \frac{\partial A_4}{\partial e} = -6J_2R_e^2\frac{nae}{p^3}\cos i$$

$$S_{43} = \frac{\partial A_4}{\partial i} = \frac{3}{2}J_2n\left(\frac{R_e}{p}\right)^2\sin i$$

$$S_{51} = \frac{\partial A_5}{\partial a} = -S_{41}\frac{5\cos^2 i - 1}{2\cos i}$$

$$S_{52} = \frac{\partial A_5}{\partial e} = -S_{42}\frac{5\cos^2 i - 1}{2\cos i}$$

$$S_{53} = \frac{\partial A_5}{\partial i} = -\frac{15}{2}J_2n\left(\frac{R_e}{p}\right)^2\sin i\cos i$$

$$S_{61} = \frac{\partial A_6}{\partial a} = -\frac{3n}{2a}\left[1 + \frac{7}{4}J_2\sqrt{1-e^2}\left(\frac{R_e}{p}\right)^2(3\cos^2 i - 1)\right]$$

$$S_{62} = \frac{\partial A_6}{\partial e} = \frac{9}{4}J_2n\left(\frac{R_e}{p}\right)^2(3\cos^2 i - 1)\frac{e}{(1-e^2)^{\frac{5}{2}}}$$

$$S_{63} = \frac{\partial A_6}{\partial i} = -\frac{9}{2}J_2n\left(\frac{R_e}{p}\right)^2\sqrt{1-e^2}\,\sin i\cos i$$

All of the other elements of $\boldsymbol{S}$ are zero.

Similarly, the elements of the $\boldsymbol{G}$ vector are found by direct differentiation of the $\boldsymbol{A}$ vector with respect to the drag factor K_D:

$$G_1 = \frac{\partial A_1}{\partial K_D} = -2\sqrt{\mu a}\,\rho_p f_1, \qquad G_2 = \frac{\partial A_2}{\partial K_D} = -\sqrt{\frac{\mu}{a}}\rho_p f_2$$

All of the other elements of $\boldsymbol{G}$ are zero.

The auxiliary functions f_1 and f_2 are

$$f_1 = \left[I_0 + 2eI_1 + (3e^2/4)(I_0 + I_2)\right]\exp(-\beta ae)$$

$$f_2 = \left\{I_1 + (e/2)[I_0 + I_2] - (e^2/8)[5I_1 + I_3]\right\}\exp(-\beta ae)$$

with the derivatives

$$\frac{\partial f_1}{\partial a} = \beta e\left[-I_0 + I_1 + 2e\left(I_0 - \frac{I_1}{\beta ae} - I_1\right) + \frac{3e^2}{4}\left(2I_1 - I_0 - I_2 - \frac{2I_2}{\beta ae}\right)\right]\exp(-\beta ae)$$

$$\frac{\partial f_1}{\partial e} = \frac{a}{e}\frac{\partial f_1}{\partial a} + \left[2I_1 + \frac{3}{2}e(I_0 + I_2)\right]\exp(-\beta ae)$$

$$\frac{\partial f_2}{\partial a} = 2\beta e\left[I_0 - I_1 - \frac{I_1}{\beta ae} + \frac{e}{2}\left(2I_1 - \frac{2}{\beta ae}I_2 - I_0 - I_2\right) - \frac{e^2}{8} \times \left(5I_0 - \frac{5}{\beta ae}I_1 + I_2 - \frac{3}{\beta ae}I_3 - 5I_1 - I_3\right)\right]\exp(-\beta ae)$$

$$\frac{\partial f_2}{\partial e} = \frac{a}{e}\frac{\partial f_2}{\partial a} + \left[I_0 + I_2 - \frac{e}{2}(5I_1 + I_3)\right]\exp(-\beta ae)$$

The functions I_n are modified Bessel functions of the first kind of the argument βae and order n. The derivatives of I_n are calculated using the relations[16]

$$\frac{\mathrm{d}I_n(z)}{\mathrm{d}z} = I_{n-1}(z) - \frac{n}{z}I_n(z), \qquad \frac{\mathrm{d}I_0(z)}{\mathrm{d}z} = I_1(z)$$

Appendix C: Relative Orbital Elements Estimation Errors

We develop expressions for the errors of the estimated orbital elements, as functions of the measurement errors of relative position and velocity. The functions are expressed as partials of the orbital elements with respect to position and velocity. The method is similar to the treatment of differential correction of orbits (as by Escobal[15]). Usually we need to write the partials of the orbital elements with respect to the three components of the position vector and the three components of the velocity vector. However, because we need these expressions only for estimation of the errors, we develop here expressions of the partials with respect to the magnitude of the measurement error of position and velocity, and we associate the direction of the measurement error with the worst-case direction. In addition, because the relative orbital elements that are relevant for the calculation of the correction velocity [Eq. (9)] are Δa, Δe, and Δi, we have to find the following six partials:

$$\frac{\partial a}{\partial r}, \frac{\partial a}{\partial V}, \frac{\partial e}{\partial r}, \frac{\partial e}{\partial V}, \frac{\partial i}{\partial r}, \frac{\partial i}{\partial V}$$

Partials of *a*

From the energy equation, we have $V^2/2 - \mu/r = -\mu/2a$. By taking the partials of a with respect to the position and velocity, we obtain

$$\frac{\partial a}{\partial r} = \frac{2a^2}{r^2}, \qquad \frac{\partial a}{\partial V} = \frac{2a^2V}{\mu}$$

For small eccentricities we have

$$\frac{\partial a}{\partial r} = 2, \qquad \frac{\partial a}{\partial V} = \frac{2a}{V}$$

Partials of *e*

Substituting $V^2 = \dot{r}^2 + (r\dot{\theta})^2$ in the energy equation, we obtain

$$\dot{r}^2 = 2\mu/r - \mu/a - (r\dot{\theta})^2$$

Substituting $\dot{\theta} = h/r^2 = \sqrt{[\mu a(1-e^2)]}/r^2$ and solving for e, we get

$$e^2 = r^2\dot{r}^2/\mu a + (1 - r/a)^2$$

From this expression we obtain the partials of e with respect to r and V:

$$\frac{\partial e}{\partial r} = \frac{1-e^2}{er}\left(\frac{a}{r} - 1\right), \qquad \frac{\partial e}{\partial \dot{r}} = \frac{r^2\dot{r}}{\mu ae}\left(1 - \frac{2a\dot{r}^2}{\mu}\right)$$

For worst-case error calculation, we assume that the measurement error of the velocity is in the radial direction, that is, $\delta V = \delta\dot{r}$.

For small eccentricities, we have, after some manipulations,

$$\frac{\partial e}{\partial r} = \frac{1}{a}, \qquad \frac{\partial e}{\partial \dot{r}} = \frac{1}{V}$$

Partials of *i*

The angular momentum vector is

$$\boldsymbol{h} = \boldsymbol{r} \times \boldsymbol{V}$$

The variation is

$$\boldsymbol{\delta h} = \boldsymbol{\delta r} \times \boldsymbol{V} + \boldsymbol{r} \times \boldsymbol{\delta V}$$

The error in the estimation of the inclination angle is associated with the error in the direction of the angular momentum vector. To get worst-case error estimation, we assume that the error of the position

vector is perpendicular to the velocity vector and parallel to the angular momentum vector, that is, $\boldsymbol{\delta r} \perp \boldsymbol{V}$ and $\boldsymbol{\delta r} \parallel \boldsymbol{h}$. Similarly, the error of the velocity vector is assumed to be perpendicular to the position vector and parallel to the angular momentum vector, that is, $\boldsymbol{\delta V} \perp \boldsymbol{r}$ and $\boldsymbol{\delta V} \parallel \boldsymbol{h}$. In addition, we assume that the estimation is performed at the nodes of the orbit; hence, the error of the direction of the angular momentum vector is the error of the inclination. Under these assumptions we get

$$h\delta i = V\delta r + r\delta V$$

The partials are then

$$\frac{\partial i}{\partial r} = \frac{V}{h}, \qquad \frac{\partial i}{\partial V} = \frac{r}{h}$$

For small eccentricity,

$$\frac{\partial i}{\partial r} = \frac{1}{a}, \qquad \frac{\partial i}{\partial V} = \frac{1}{V}$$

References

[1]Bristow, J., Folta, D., and Hartman, K., "A Formation Flying Technology Vision," AIAA Paper 2000-5194, Sept. 2000.

[2]Schaub, H. S., and Alfriend, K. T., "J_2 Invariant Reference Orbits for Spacecraft Formation," *Celestial Mechanics and Dynamical Astronomy*, Vol. 79, No. 2, 2001, pp. 77–95; also Paper 11, Flight Mechanics Symposium, Goddard Space Flight Center, Greenbelt, Maryland, 18–20 May 1999.

[3]Schaub, H. S., Vadali, S. R., Junkins, J. L., and Alfriend, K. T., "Spacecraft Formation Flying Control Using Mean Orbit Elements," *Journal of Astronautical Sciences*, Vol. 48, No. 1, 2000, pp. 69–87; also American Astronautical Society, Paper AAS 99-310, Aug. 1999.

[4]Schaub, H. S., and Alfriend, K. T., "Impulsive Feedback Control to Establish Specific Mean Orbit Elements of Spacecraft Formations," *Journal of Guidance, Control, and Dynamics*, Vol. 24, No. 4, 2001, pp. 739–745.

[5]Vadali, S. R., Vaddi, S. S., Naik, K., and Alfriend, K. T., "Control of Satellite Formations," AIAA Paper 2001-4028, Aug. 2001.

[6]Folta, D., and Quinn, D., "A Universal 3-D Method for Controlling the Relative Motion of Multiple Spacecraft in Any Orbit," Paper AIAA 98-4193, Aug. 1998.

[7]Mishne, D., "Relative Formation Keeping of LEO Satellites Subject to Small Drag Differences," American Astronautical Society, Paper AAS 01-455, Aug. 2001.

[8]Carter, T., and Humi, M., "Clohessy–Wiltshire Equations Modified to Include Quadratic Drag," *Journal of Guidance, Control, and Dynamics*, Vol. 25, No. 6, 2002, pp. 1058–1063.

[9]Sabol, R., Burns, D., and McLaughlin, C. A, "Satellite Formation Flying Design and Evolution," *Journal of Spacecraft and Rockets*, Vol. 38, No. 2, 2001, pp. 270–278.

[10]Vallado, D. A., *Fundamentals of Astrodynamics and Applications*, McGraw–Hill, New York, 1997, pp. 561–567, 606.

[11]Kwakernaak, H., and Sivan, R., *Linear Optimal Control Systems*, Wiley-Interscience, New York, 1972, pp. 12, 13.

[12]How, J. P., and Tillerson, M., "Analysis of the Impact of Sensor Noise on Formation Flying Control," *Proceedings of the American Control Conference*, IEEE Press, Piscataway, NJ, 2001, pp. 3986–3991.

[13]Imre, E., Palmer, P., and Hashida, Y., "Precise Relative Orbit Determination of Low Earth Orbit Formation Flights Using GPS Pseudorange and Carrier-Phase Measurements," Paper SSC02-IV-1, 16th Annual AIAA/Utah State Univ. Conf. on Small Satellites, Aug. 2002.

[14]Busse, F. D., and How, J. P., "Real-Time Experimental Demonstration of Precise Decentralized Relative Navigation for Formation Flying Spacecraft," AIAA Paper 2002-5003, Aug. 2002.

[15]Escobal, P. R., *Methods of Orbit Determination*, Krieger, Malabar, FL, 1976, pp. 318–339.

[16]Abramowitz, M., and Stegun, I. A., *Handbook of Mathematical Functions*, Dover, 1970, pp. 374–376.